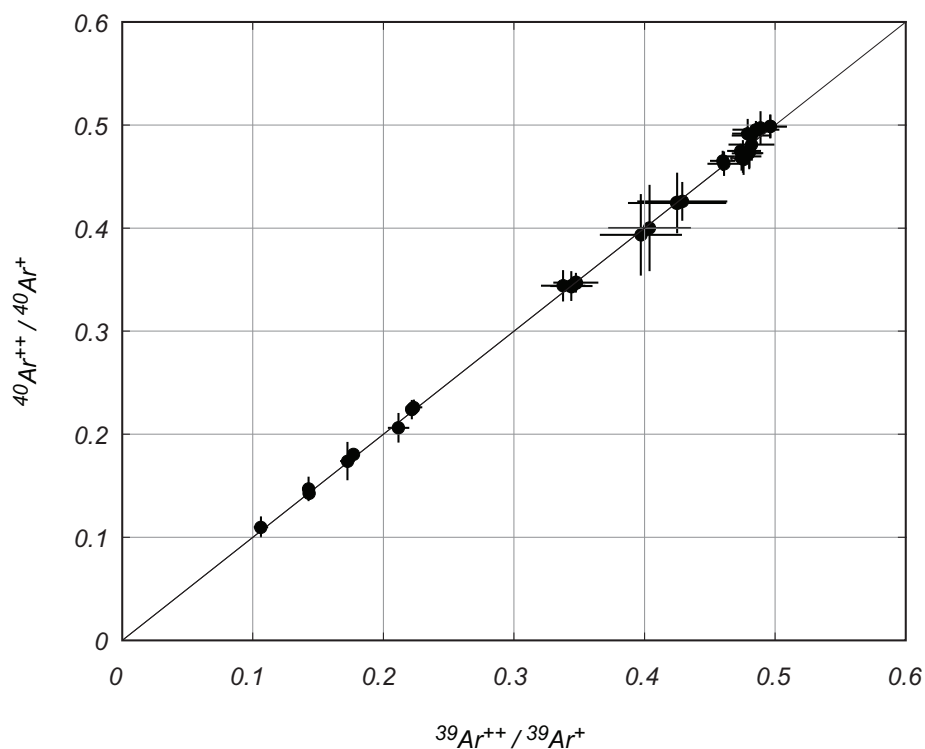
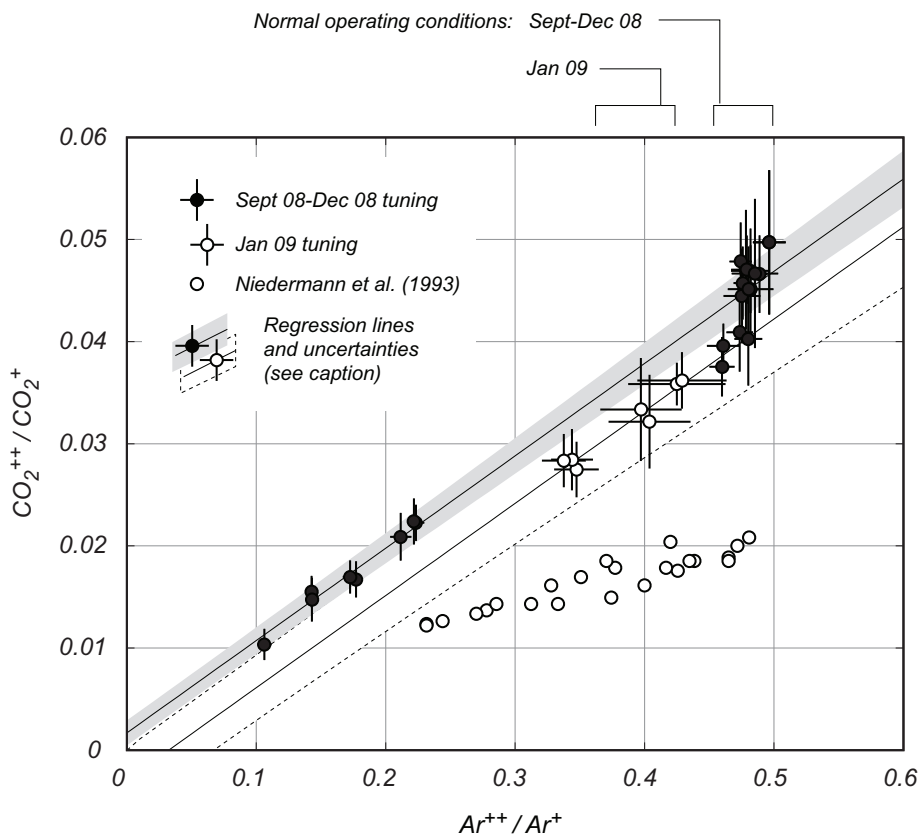


Supplementary data accompanying Balco and Shuster, ‘Production rate of cosmogenic  $^{21}\text{Ne}$  in quartz estimated from  $^{10}\text{Be}$ ,  $^{26}\text{Al}$ , and  $^{21}\text{Ne}$  concentrations in slowly eroding Antarctic bedrock surfaces.’



**Figure S1.** Ratio of doubly- to singly-charged Ar inferred from measurements on masses 19.5/39 ( $^{39}\text{Ar}^{++}/^{39}\text{Ar}^+$ ) and 20/40 ( $^{40}\text{Ar}^{++}/^{40}\text{Ar}^+$ ). We made these measurements by introducing only the  $^{39}\text{Ar}$  spike, and no Ne, into the mass spectrometer.  $^{40}\text{Ar}$  is present as background. The charge ratio varied somewhat under normal operating conditions, and we achieved a larger range of variability by adjusting the temperature of a SAES getter in the source, thus changing the partial pressure of hydrogen.  $^{40}\text{Ar}$  The dark line shows a 1:1 relationship.



**Figure S2.** Relationship between double/single charge ratios for Ar and  $CO_2$ . We made these measurements by introducing only the  $^{39}Ar$  spike, and no Ne, into the mass spectrometer, then measuring on masses 19.5/39 ( $^{39}Ar^{++}/^{39}Ar^+$ ) and 22/44 ( $CO_2^{++}/CO_2^+$ ).  $CO_2$  is present as background. During normal operating conditions, both charge ratios varied over only a relatively small range. In order to obtain a wider range of charge ratios and a more accurate regression, we varied the temperature of a SAES getter in the source, which presumably affected the charge ratios via the partial pressure of hydrogen. During a Ne measurement, we measured the  $Ar^{++}/Ar^+$  ratio by monitoring masses 19.5 and 39, then using the regression line shown here to estimate the  $CO_2^{++}/CO_2^+$  ratio. The open circles without error bars show similar measurements from Niedermann et al. (1993). They presented these as relationships between double/single charge ratios and the  $H_2$  signal in the mass spectrometer; we have replotted them here to show that they also observed a linear relationship between the Ar and  $CO_2$  charge ratios.

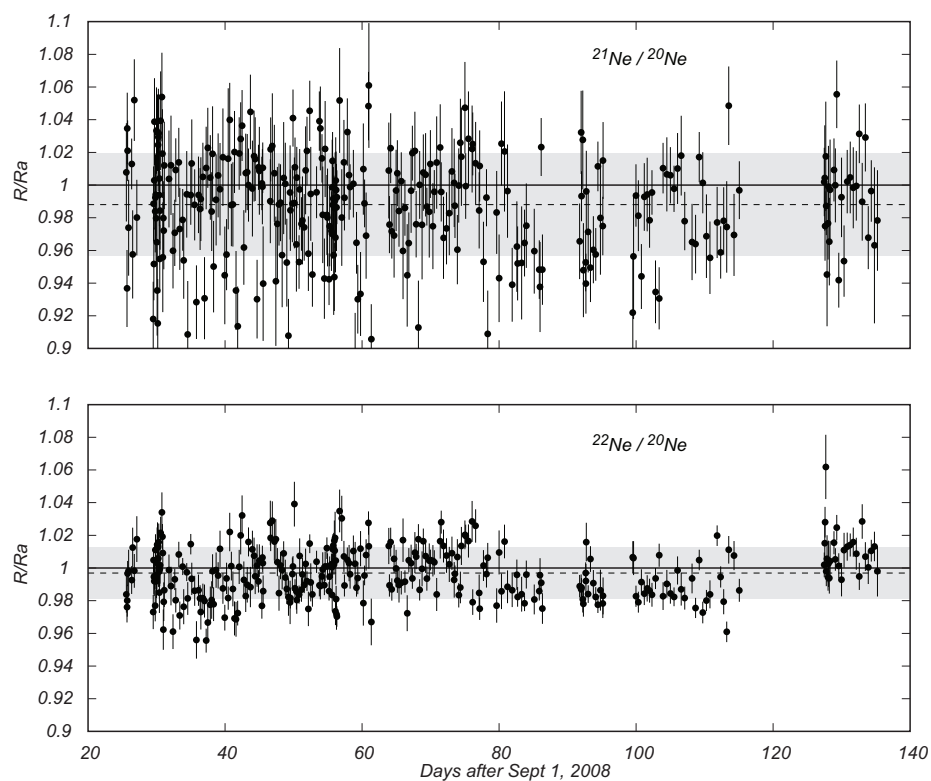


**Figure S3.** Ne isotope ratios of air pipettes analyzed during the period in which we made the measurements in this paper. The y-axis shows the ratio of the measured isotope ratio to the accepted atmospheric ratio ( $^{21}\text{Ne}/^{20}\text{Ne} = 0.002959$ ;  $^{22}\text{Ne}/^{20}\text{Ne} = 0.1020$ ). The dotted black line and gray band show the mean and one standard deviation of all measurements.

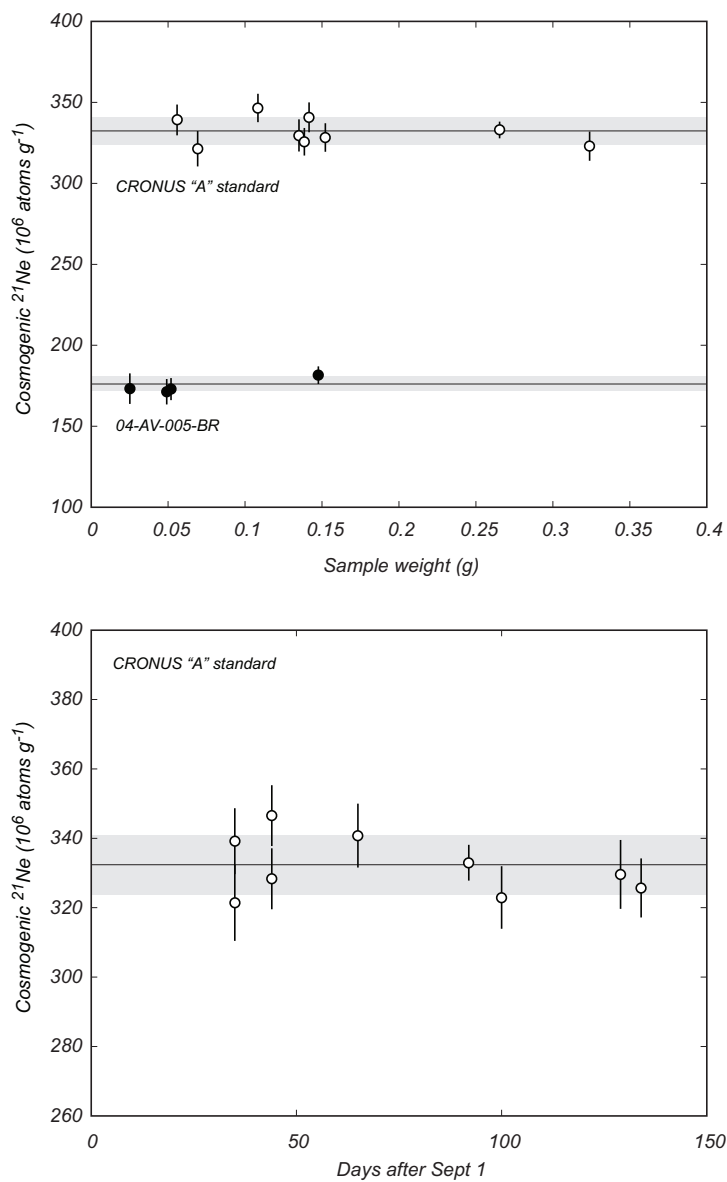


**Figure S4.** Linearity and reproducibility over time of multiple analyses of separate aliquots of the same quartz sample. We used the CRONUS 'A' quartz standard as an internal standard and measured it repeatedly with both laser and resistance furnace extraction systems; the individual measurements are shown in Table S1. The dark lines and grey bands show the error-weighted means and  $1\sigma$  uncertainties of all measurements.

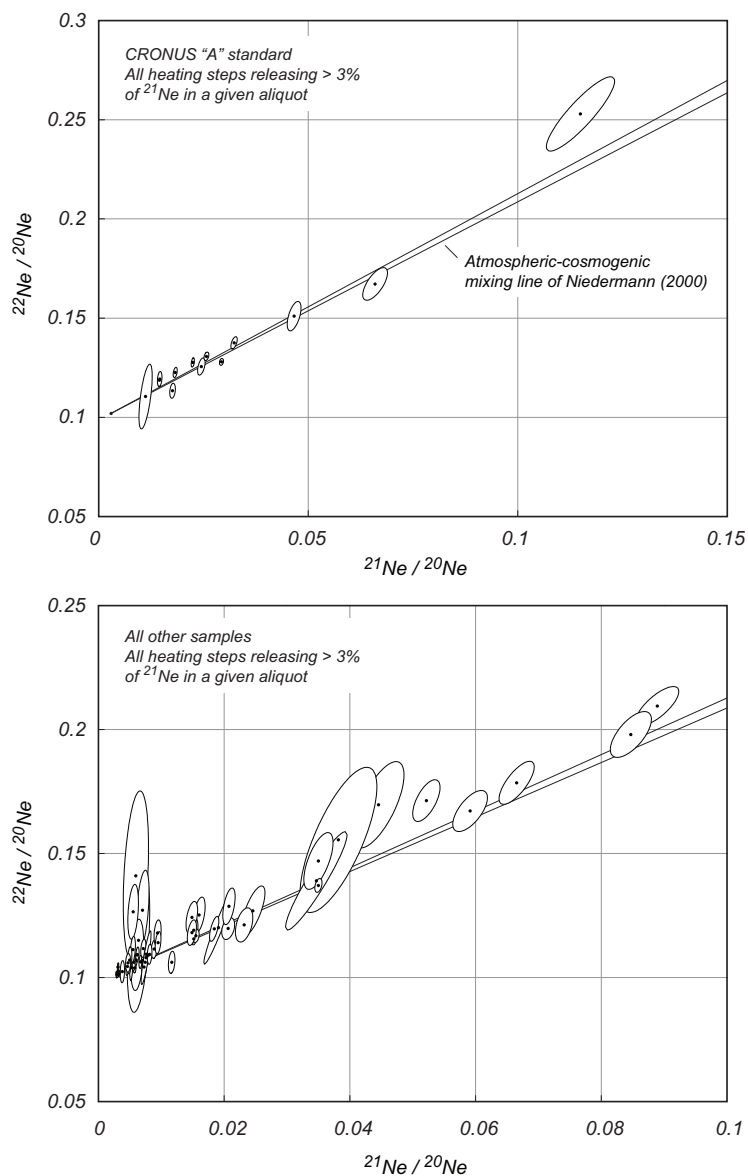


**Figure S5.** Ne isotope compositions of samples analyzed in this study as well as the CRONUS 'A' standard that we used as an internal standard. The dark line in both figures is the atmospheric-cosmogenic mixing line (Niedermann, 2000; the width of the line reflects the  $1\sigma$  uncertainty in its slope stated in that paper). Only heating steps that released more than 3% of the total cosmogenic  $^{21}\text{Ne}$  in a particular aliquot are shown. In both panels, the ellipses are 68% confidence regions.